Histochemistry (1987) 87:393–406

Histochemistry

1,25 $(OH)_2$ vitamin D_3 sites of action in the brain

An autoradiographic study

W.E. Stumpf and L.P. O'Brien
Departments of Anatomy and Pharmacology, University of North Carolina, 534 Swing Building, Chapel Hill, NC 27514, USA

Accepted June 17, 1987

Summary. After injection of ^3H 1,25 $(OH)_2$ vitamin D_3 to adult rats and mice, under normal or vitamin D deficient diet, the hormone was found to be accumulated in nuclei of neurons in certain brain regions. Nuclear concentration was prevented or diminished, when excess unlabeled 1,25 $(OH)_2$ vitamin D_3 was injected before ^3H 1,25 $(OH)_2$ vitamin D_3, while excess 25 (OH) vitamin D_3 did not prevent nuclear labeling.

Highest nuclear concentration of ^3H 1,25 $(OH)_2$ vitamin D_3 is observed in certain neurons in the nucleus interstitialis striae terminalis, involving its septo-preoptic pars dorsolateralis and its anterior hypothalamic-thalamic portion, and in the nucleus centralis of the amygdala, all constituting a system of target neurons linked by a component of the stria terminalis. Nuclear concentration of ^3H 1,25 $(OH)_2$ vitamin D_3 is also found in neurons in the periventricular nucleus of the preoptic-hypothalamic region, including its extensions, the parvocellular paraventricular and arcuate nucleus, in the ventromedial nucleus, supramammillary nucleus, reticular nucleus of the thalamus, ventral hippocampus, caudate nucleus, pallium, in the midbrain-pontine central gray, dorsal raphe nucleus, parabrachial nuclei, cranial motor nuclei, substantia gelatinosa of the sensory nucleus of the trigeminus, Golgi type II cells of the cerebellum, and others.

The extensive distribution of target neurons suggests that 1,25 $(OH)_2$ vitamin D_3 regulates the production of several aminergic and peptidergic messengers, and influences the activity of certain endocrine-autonomic, sensory and motor systems.

Introduction

Evidence for nuclear binding of 1,25 dihydroxyvitamin D_3 (1,25 D_3; calcitriol) to cells in the nervous system was first obtained in our laboratory for pituicytes in the posterior pituitary (Stumpf et al. 1979) and for certain neuronal groups in the forebrain, hindbrain, and spinal cord (Stumpf et al. 1980, 1981a). In conjunction with other new findings of vitamin D targets, which include, thyrotropes in the anterior pituitary (Stumpf et al. 1979; Sar et al. 1980), endocrine gastrin-producing cells in the antrum of the stomach (Stumpf et al. 1979), and B-cells in the endocrine pancreas (Clark et al. 1980), the concept of a vitamin D-related brain-pituitary endocrine axis analogous to other steroid hormones was proposed (Stumpf et al. 1982). Since then, other endocrine tissues have been discovered as targets for 1,25 D_3, such as, adrenal medullary cells (Clark et al. 1986), Sertoli cells in the testis (Stumpf et al. 1987b), and thyroid follicle epithelial cells (Stumpf and O'Brien 1987), some of which may be under additional 1,25 D_3-mediated neuroendocrine control.

Despite the autoradiographic data published six years ago, no evidence for nuclear receptors has yet been obtained through biochemical assays (Colston et al. 1980). A "limited apparent uptake" for (^3H)1,25 D_3 in canine and rodent brain has been reported, although it was suggested that the hormone does not penetrate freely into the brain (Gascon-Barré and Huet 1983). Supportive of the presence of 1,25 D_3 receptors in brain, is a recent report on 1,25 D_3 mediated elevation of choline acetyltransferase activity in regions of the arcuate nucleus-median eminence and the bed nucleus of the stria terminalis, while calcium binding protein and monoamine oxidase activity measured in discrete brain regions remained unchanged (Sonnenberg et al. 1986).

The present autoradiographic studies were conducted to provide a more extensive and detailed mapping of the central nervous system sites of nuclear binding of 1,25 D_3. The results contribute information that is necessary for an understanding of central actions of calcitriol. Also, the results provide a basis for further histochemical studies, so that chemistry and function of the target cells can be characterized. Detailed topographic knowledge not only gives clues as to the mode of action of the agent, it is prerequisite for further explorations aimed at clarification of the related physiology, pharmacology, and pathology.

Materials and methods

Adult male Holtzman Sprague-Dawley rats ($n=7$), one male and one female Swiss-Webster mouse were used. One rat and the 2 mice were fed a normal rodent chow (D+), the other animals were fed a vitamin D-deficient diet (D−), supplemented with vitamin A, E, and K, for 4 weeks before the experiment. [26, 27-^3H] 1,25 OH_2 vitamin D_3, specific activity 160 Ci/m*M* dissolved in ethanol-isotonic saline, was injected intravenously to rats, 0.05–0.4 μg/100 g b.w., or subcutaneously to Swiss Webster mice, 0.38 μg/100 g b.w. The latter was divided into 2 doses administered at 1 h intervals.

In competition studies, 2 of the D− rats were injected i.v. 30 min before ^3H 1,25 D_3 with 10 μg of the unlabeled hormone, or of unlabeled 25 (OH) vitamin D_3. After the injection of the

radiolabeled hormone, the rats were decapitated at 2 h and the mice at 3–4 h.

Brain, pituitary and duodenum as control target tissues, were dissected, mounted and frozen onto tissue holders in liquefied propane at −180° C and subsequently stored in liquid nitrogen. 4-µm sections were cut in a cryostat (Jung Frigocut, Heidelberg). The frozen sections were thaw-mounted onto photographic emulsion (Kodak NTB 3)-coated slides and exposed in lightproof desiccator boxes at −20° C for different lengths of time. After the photographic exposure, slides were fixed for 30 s in 2.5% paraformaldehyde in 0.01 *M* phosphate-buffered saline. The slides were then rinsed in tap water, developed in Kodak D-19 developer (diluted 1:1) for 1 or 2 min, rinsed, and then fixed in Kodak fixer for 4 min, rinsed again, and then stained with methylgreen-pyronin. The thaw-mount autoradiographic technique, which was developed in our laboratory (Stumpf and Roth 1966), has been described in detail (Stumpf 1976).

From each region 5–10 cells with the highest number of nuclear silver grains and with the highest nuclear diameter (cut through the center of the nucleus) were quantitated with the aid of an automated silver grain counter (Artek Counter, Model 982, Farmingdale, New York). Exposure times were selected for individual regions, so that silver grains were accumulated but not clustered and could be counted individually. With the help of a computer program that considers the specific activity of the radiolabeled compound, exposure time, and silver grain yield, the number of radiolabeled molecules per nucleus was computed as detailed (Stumpf et al. 1981b). It is assumed that all or most of the radioactivity that is retained in nuclei represents the original compound.

Results

After injection of ^{3}H calcitriol, radioactivity is concentrated in certain structures in the brain of rats and mice, in D− and in D+ animals. At the different time intervals studied, radioactivity is found throughout the brain, without a perivascular or periventricular gradient, that is, without indication of impaired penetration. Radioactivity is high in lumina of blood vessels and in choroid plexus, while there are varying low levels in the neuropil and nerve tracts. Radioactivity is concentrated in the nucleus of certain neurons in select regions throughout the brain. The intensity of nuclear concentration of radioactivity varies among neurons of the same region and among different neuronal groups. Correspondingly, after short autoradiographic exposure times or administration of low doses of radiolabeled hormone, only regions and neurons with relatively high nuclear labeling are recognized, while after long exposure times or administration of high doses of radiolabeled compound, additional regions and neurons with low nuclear concentration of radioactivity become apparent. Animals that were injected with a high single dose, or received two pulses, of ^{3}H calcitriol and were fed a normal diet, showed the most extensive and intensive nuclear neuronal labeling pattern. With these animals, results were obtained at a shorter autoradiographic exposure time than with animals that received a low dose and that were fed a vitamin D-deficient diet. Differences in the extent of nuclear labelling may also be related to age and the endocrine status of the animals. The limited number of animals, however, does not permit establishing select interrelations. In general, in the low-dose animals nuclear labeling of neurons is seen consistently in the central nucleus of the amygdala and in the bed nucleus of the stria terminalis (Figs. 1 and 2). These may be the only detectable labeled sites in the forebrain of some of these animals. In some of these animals nuclear labeling is weak, or not apparent in regions, such as, the piriform cortex, caudate-putamen, dorsal raphe, and Golgi type II cells in the granular layer of the cerebellum. Cells with nuclear concentration of radioactivity that contain a number of nuclear silver grains more than twice the number of silver grains over adjacent corresponding tissue, are considered labeled. Labeled cells are neurons of different size. Glial cells, with the exception of certain pituicytes, do not appear to be labeled. In nuclei of large motor neurons of cranial nerves and of lamina IX in the spinal cord, the intense labeling after long exposure times may reveal a distinct negative region that stains red for RNA with methylgreen-pyronin and represents the nucleolus. In many of the unlabeled large neurons in the reticular formation or in the nucleus of the mesencephalic tract of the trigeminus the radioactivity in the nucleus appears lower than in the cytoplasm.

When excess unlabeled calcitriol was injected before the injection of tritiated calcitriol, no nuclear concentration of radioactivity is observed. When excess unlabeled 25 (OH) vitamin D_3 was injected before ^{3}H 1,25 D_3, nuclear labeling is apparent, similar to the animals that received ^{3}H 1,25 D_3 alone.

Examples of autoradiograms are provided in Figs. 1–32. A survey of labeled neurons, as seen in autoradiograms of high dose animals, is depicted schematically (Fig. 33) on representative frontal planes in a rostro-caudal sequence.

At the level of the septum, the septal nuclei, the nucleus of the diagonal band, and the nucleus accumbens appear essentially free of labeled cells. In the nucleus accumbens, one labeled cell has been seen dorsal to the root of the anterior commissure. In the caudate-putamen, scattered weakly labeled neurons exist especially in its ventrolateral part, while its medial portions are mostly free of labeled cells. This pattern exists throughout the rostro-caudal extent of the caudate-putamen. In the cortex, scattered labeled neurons of varying labeling intensity can be found in all laminae, rare in the cingulate cortex, and relatively frequent in laminae 3 and 4 in the adjacent dorsal and dorsolateral isocortex, while ventral to the rhinal sulcus in the piriform cortex labeled cells are most numerous (Fig. 16). A cluster of labeled cells exists immediately ventral to the rhinal sulcus, especially in laminae 2 and 3. Labeled cells diminish in number and are scattered ventrally in the piriform cortex toward the region dorsal to the lateral olfactory tract rostrally and the transition to the amygdala more caudally. This pattern of distribution of labeled neurons can be followed throughout the cerebral hemisphere (Figs. 12 and 13). Occasionally, labeled neurons can be seen in deeper cortical layers, notably immediately adjacent to the corpus callosum. A few labeled cells are observed even within the corpus callosum.

In the bed nucleus of the stria terminalis, heavily labeled cells are conspicuous in its dorsolateral subventricular subnucleus at the preoptic and thalamic-anterior hypothalamic levels (Figs. 1 and 9). This group of labeled neurons extends rostro-ventrally into the lateral hypothalamus, where a small number of heavily labeled neurons border the capsula interna.

In the preoptic region, labeled neurons are also present in the nucleus periventricularis. Labeled cells can be seen throughout the hypothalmic periventricular nucleus (Figs. 3–7), most frequently in the anterior hypothalamic region. These labeled cells constitute a component of the

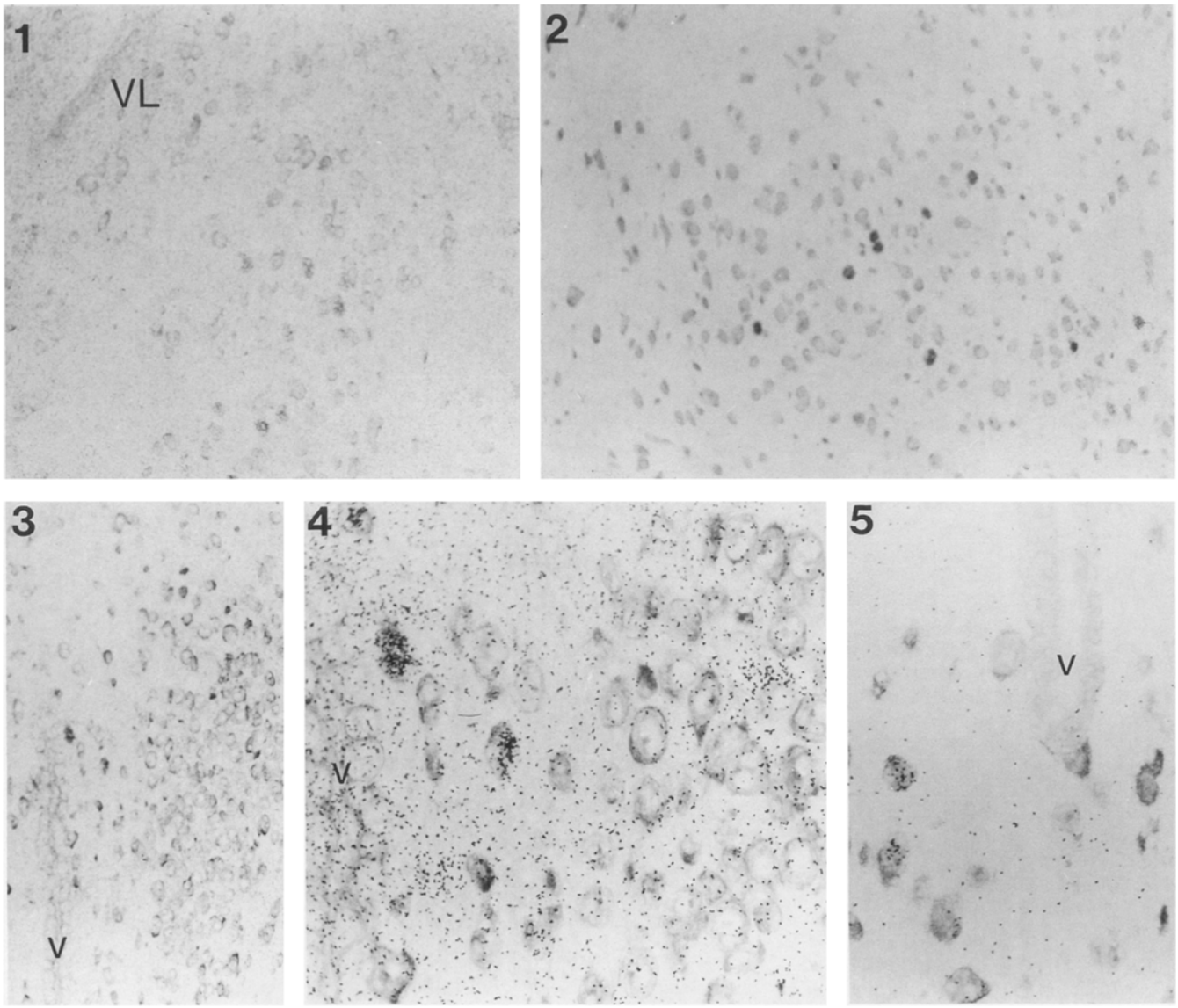

Figs. 1–32. Autoradiograms of mouse forebrain (**Figs. 1–18**) and hindbrain (**Figs. 19–32**) after injection of ^{3}H 1,25 $(OH)_2$ vitamin D_3, demonstrating nuclear concentration of radioactivity in neurons. 4-μm frontal sections, stained with methylgreen-pyronin

Figs. 1–5. In preoptic and anterior hypothalamic regions, strongest nuclear labeling is seen in the nucleus of the stria terminalis pars dorsolateralis at the level of the anterior commissure between the tip of the lateral ventricle (*VL*) and the caudate nucleus (**Fig. 1**), and in the central nucleus of the amygdala (**Fig. 2**). Also, neurons of the periventricular nucleus (**Figs. 3–5**), including the parvocellular but not the magnocellular portion of the paraventricular nucleus, are labeled. **Fig. 3** (*low power*) and **Fig. 4** (*high power*) show labeled neurons at dorsal aspect of third ventricle (*V*) medial to unlabeled neurons of the magnocellular paraventricular nucleus. In **Fig. 5** labeled neurons are seen at ventral extent of third ventricle. Exposure: 448 days (**Figs. 3–4**), 360 days (**Fig. 1**), 321 days (**Fig. 5**), 175 days (**Fig. 2**). Magnification: ×175 (**Figs. 1–3**), ×551 (**Figs. 4–5**)

parvocellular paraventricular nucleus (Figs. 3 and 4), while cells of the magnocellular paraventricular nucleus are unlabeled. In this region, labeled cells are relatively numerous in the ventral periventricular nucleus and subventricularly in the rostral extent of the arcuate nucleus.

At the level of the central hypothalamus, labeled neurons are present especially in and near the periventricular region of the dorsal arcuate nucleus (Fig. 7). Occasionally, a labeled cell is noted in more central parts of the arcuate nucleus, including its rostral subventricular and its central and caudal portions. The ventromedial nucleus, like most of the arcuate nucleus, is free of labeled cells, with the exception of one or two labeled cells in its ventral part, as seen in a few of the sections (Fig. 8). In the amygdala, heavily labeled cells are conspicuous in the central nucleus (Fig. 2), while the other nuclei are unlabeled, with the exception of an occasional single labeled cell in the vicinity of the massa intercalata. In the lateral thalamus, cells of the reticular nucleus show strong labeling (Fig. 10).

At the level of the caudal hypothalamus, a few labeled cells are observed in the dorsal lateral hypothalamus and in the supramammillary nucleus (Fig. 11).

The hippocampus in most parts is free of labeled cells, except in the hippocampus inferior. In the caudal ventral hippocampus, area CA4 contains an accumulation of labeled pyramidal cells (Figs. 15 and 18). The region of la-

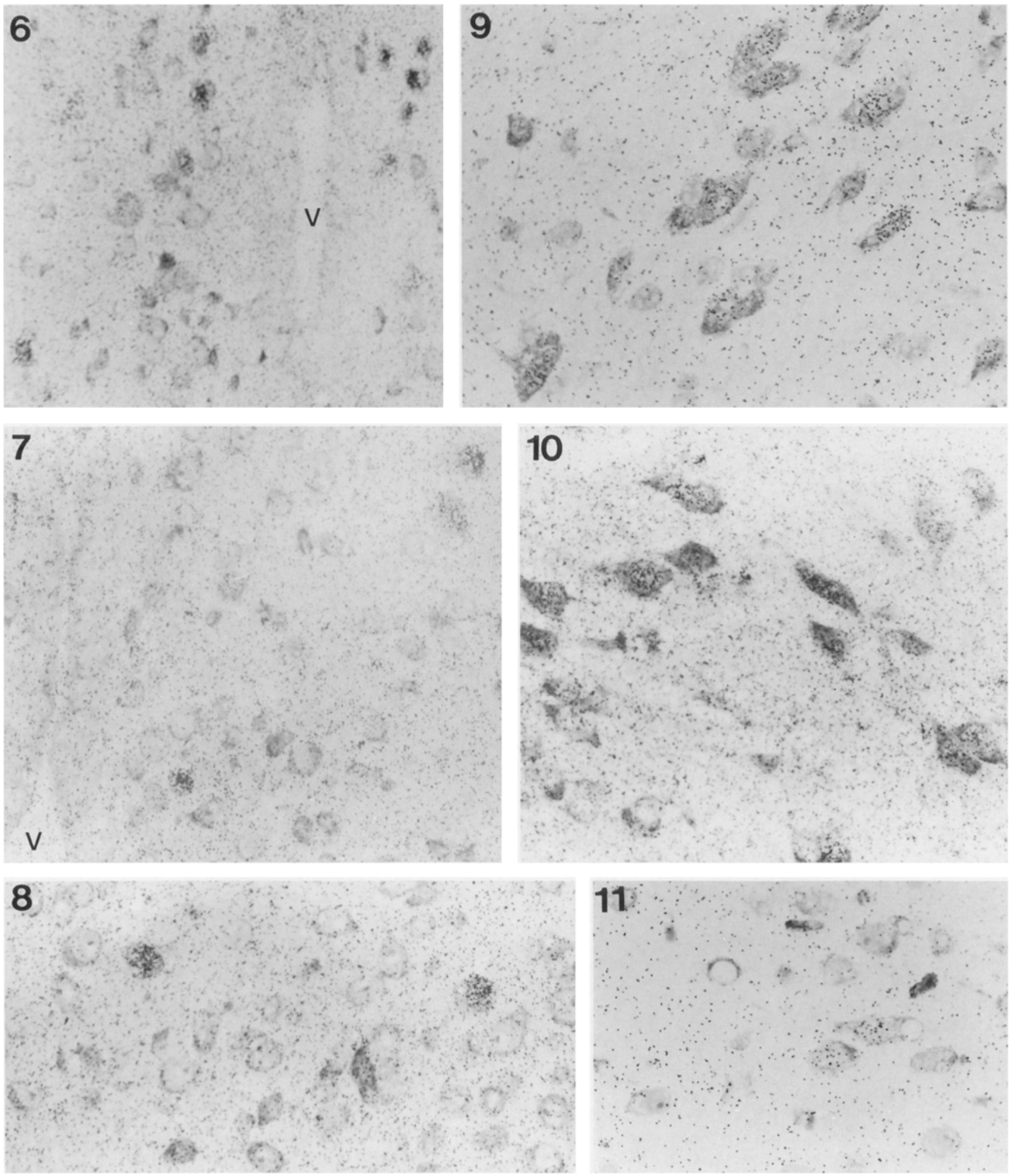

Figs. 6–11. In central hypothalamus and thalamus scattered labeled neurons are present in the periventricular nucleus (**Figs. 6**, *V* = 3rd ventricle) and dorsal arcuate nucleus (rostral portion, Fig. 6 and at level of median eminence, **Fig. 7**), in the ventromedial nucleus (**Fig. 7**, upper right; **Fig. 8**), and in the supramammillary nucleus (**Fig. 11**). Labeled neurons are numerous in the thalamic portion of the bed nucleus of the stria terminalis (**Fig. 9**) and in the reticular nucleus of the thalamus (**Fig. 10**). Exposure: 448 days (**Figs. 6–8, 10**), 321 days (**Fig. 9**), 176 days (**Fig. 11**). Magnification: ×551 (**Figs. 9 and 11**), ×438 (**Figs. 7–8, 10**), ×350 (**Fig. 6**)

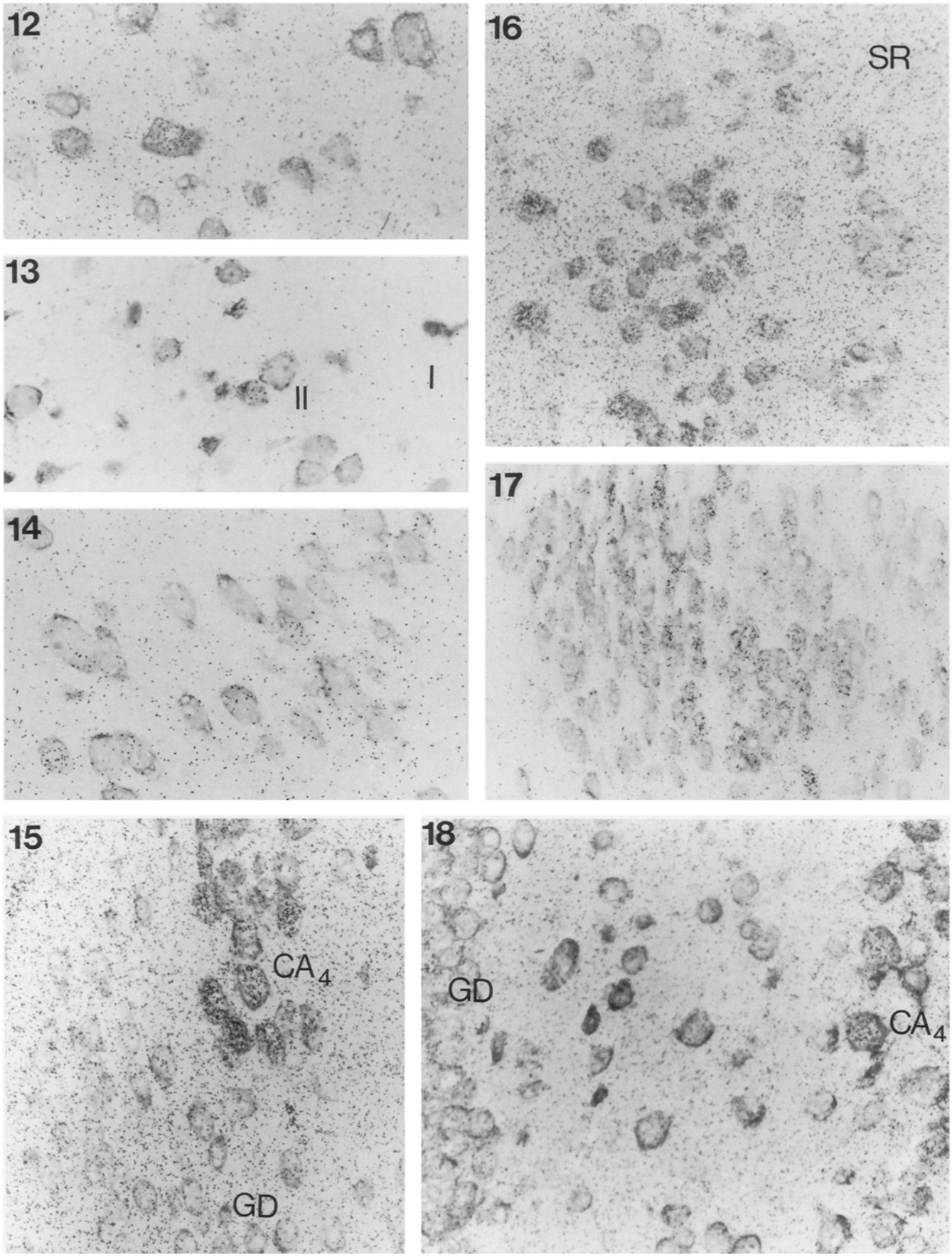

Figs. 12–18. In neocortex and allocortex target neurons for 1,25 D_3 are scattered in many regions, for example, in parietal cortex lamina V (**Fig. 12**) and lamina II (**Fig. 13**), in entorhinal cortex (**Fig. 14**), and especially in piriform cortex (**Fig. 16**), where clusters of labeled neurons exist immediately ventral to the rhinal sulcus (*SR*). In the ventral caudal hippocampus labeled neurons are found in *CA4* (**Figs. 15 and 18**), while neurons of the adjacent dentate gyrus (*GD*) are unlabeled. In the presubiculum (**Fig. 17**) exists a dense group of labeled neurons. Exposure: 448 days (**Figs. 15 and 18**), 321 days (**Figs. 14 and 17**), 232 days (**Figs. 12 and 16**), 82 days (**Fig. 13**). Magnification: ×551 (**Figs. 12–14**), ×438 (**Figs. 15–18**)

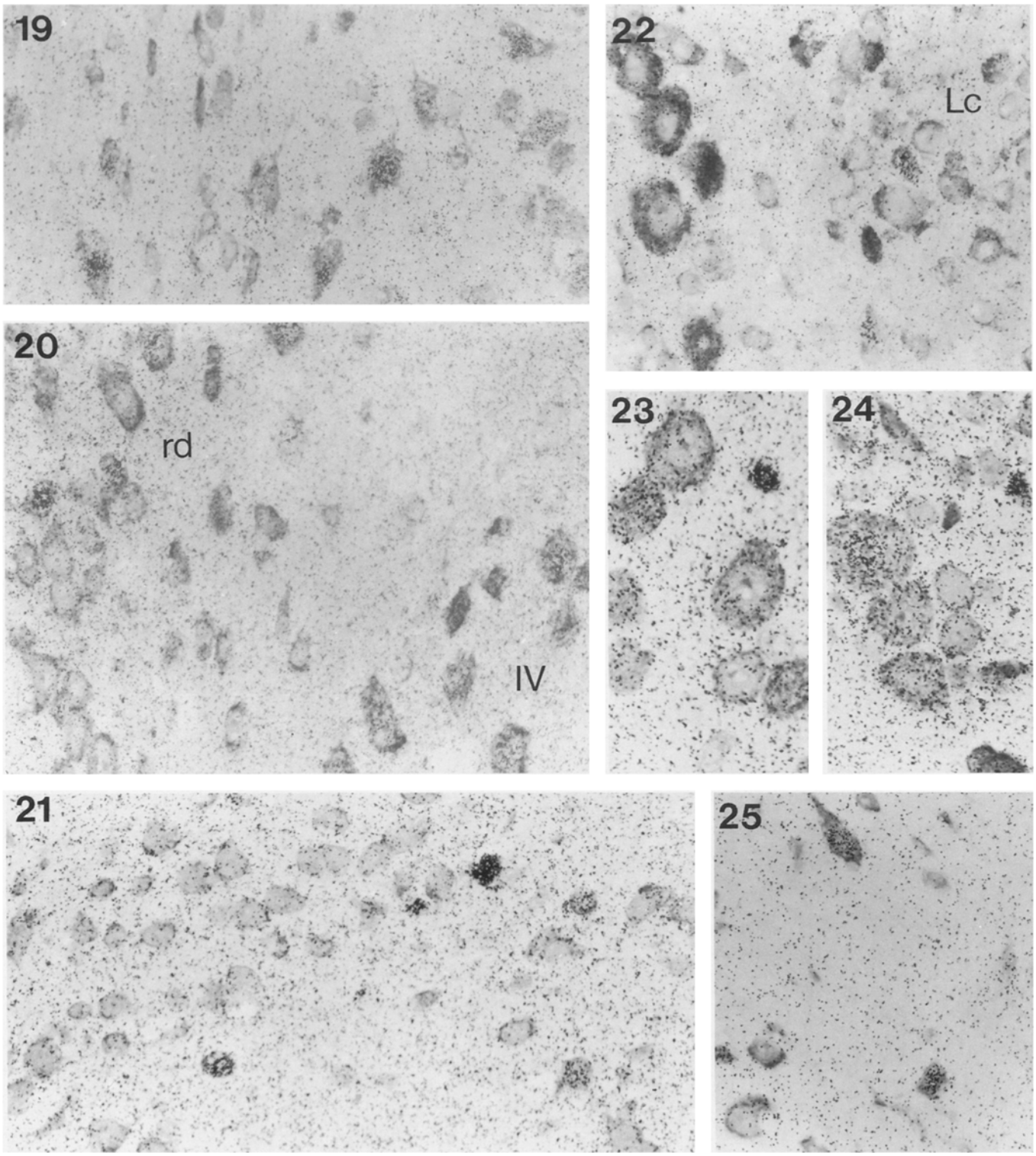

Figs. 19–25. In midbrain and pons, labeled neurons exist in n. oculomotorius (**Fig. 19**, close to the midline), n. raphe dorsalis (*rd*) and n. trochlearis (IV) (**Fig. 20**), lateral (**Fig. 21**) and medial (**Fig. 25**) parabrachial nuclei, among unlabeled neurons in locus ceruleus (**Fig. 22,** *Lc*) and in n. of the mesencephalic tract of the trigeminus (**Figs. 23 and 24**). On occasion, a characteristic large neurons of the trigeminal mesencephalic tract nucleus shows nuclear concentration of radioactivity (**Fig. 24**), while in many of the other large neurons high levels of radioactivity are observed in the cytoplasm, surrounding a nucleus which is devoid of or has distinctly low levels of radioactivity. Exposure: 365 days (**Figs. 19–20, 22**), 320 days (**Figs. 21, 23–25**). Magnification: ×551 (**Figs. 20, 23–25**), ×438 (**Figs. 19, 21–22**)

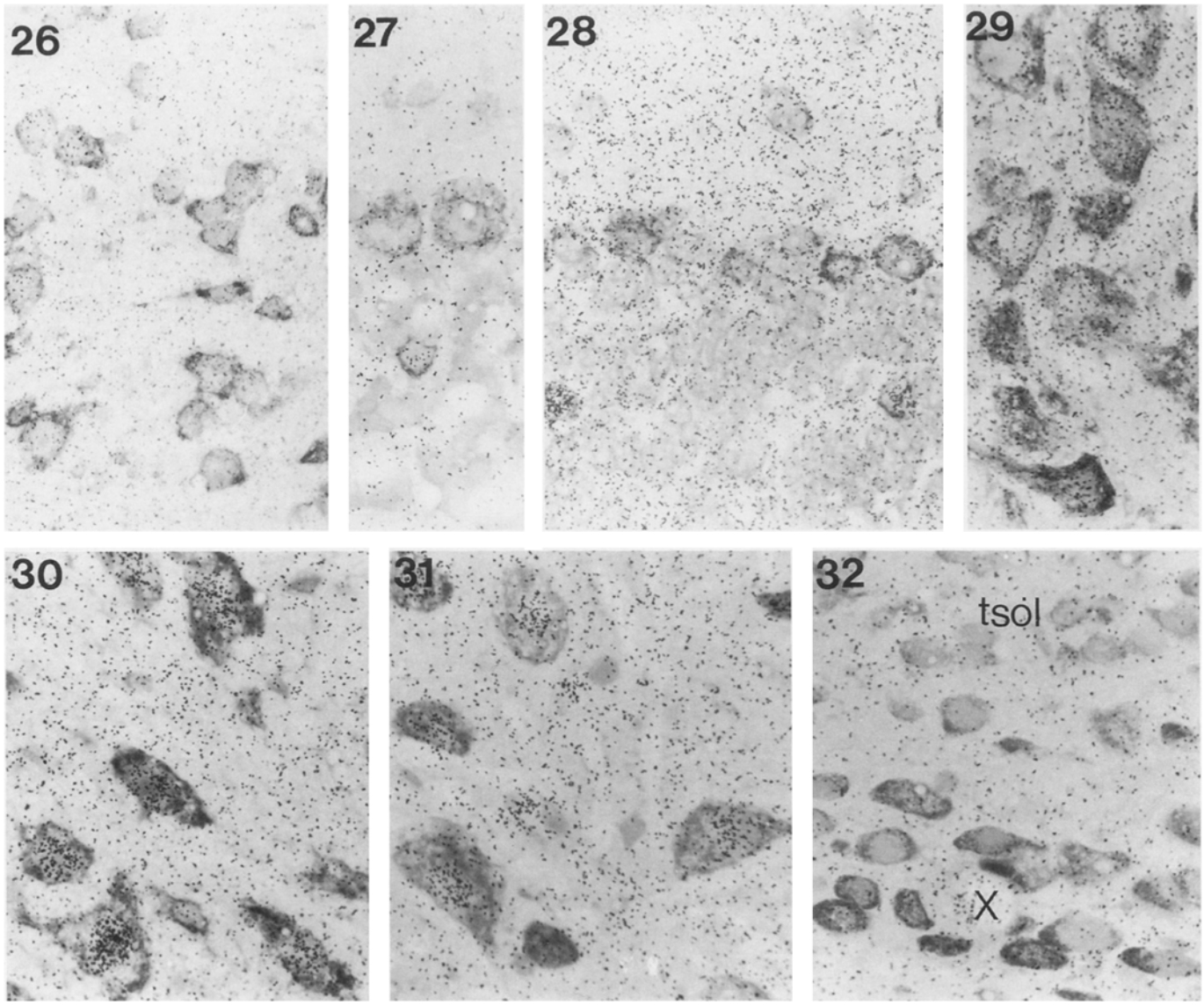

Figs. 26–32. In the nucleus pontis, scattered weakly labeled cells are present (**Fig. 26**). In cerebellum, Golgi type II cells are labeled, while Purkinje cells, granule cells, and stellate cells do not show nuclear accumulation of radioactivity in male low dose (**Fig. 27**) and female high dose (**Fig. 28**) mouse. Weak nuclear labeling in neurons of n. ambigous (**Fig. 29**), but strong nuclear radioactivity in motor neurons of n. trigeminus (**Fig. 30**) and n. hypoglossus (**Fig. 31**), while neurons of n. vagus (*X*) and n. solitary tract (*tsol*) (**Fig. 32**) are unlabeled. Exposure: 320 days (**Figs. 29–32**), 365 days (**Figs. 26–28**). Magnification: ×551 (**Figs. 27–32**), ×438 (**Fig. 26**)

beled cells may include a portion of the adjacent area CA3. A group of labeled cells is also seen in the presubiculum (Fig. 17), that is the transition area between hippocampus and entorhinal cortex. In the entorhinal cortex, scattered labeled cells exist and are continuous with the labeled cells in the piriform cortex.

In the midbrain-hindbrain region, the strongest nuclear labeling is seen in neurons of the nucleus oculomotorius (Fig. 19), trochlearis (Fig. 20), motorius trigeminus (Fig. 30), facialis, and hypoglossus (Fig. 31). In the midbrain central gray, on occasion a single labeled cell is found, dorsal and ventrolateral to the aqueduct. In the nucleus raphes dorsalis (Fig. 20), a subpopulation of 15%–20% of the cells is labeled with medium to high intensity. Throughout the nucleus pontis (Fig. 26), scattered labeled cells are present. The labeling is weak, and in several of the cells, the nuclear radioactivity is only slightly above background. On both sides of the pedunculus cerebelli superior in the region of the lateral and medial parabrachial nucleus (Figs. 21 and 25), as well as within the pedunculus, scattered small to medium-sized strongly labeled cells exist. A few of such cells are present also in the locus ceruleus (Fig. 22), in the nucleus tractus mesencephalicus nervi trigemini (Figs. 23 and 24), and in the subceruleal area. Cells in the locus ceruleus are otherwise unlabeled. Among the unlabeled large neurons of the nucleus of the mesencephalic tract of the trigeminus, a few of the large cells display a nuclear concentration of radioactivity (Fig. 24). In most of the large neurons of this nucleus, a nuclear concentration is not only absent, but the nuclear radioactivity appears distinctly lower than the radioactivity in the surrounding cytoplasm (Fig. 23).

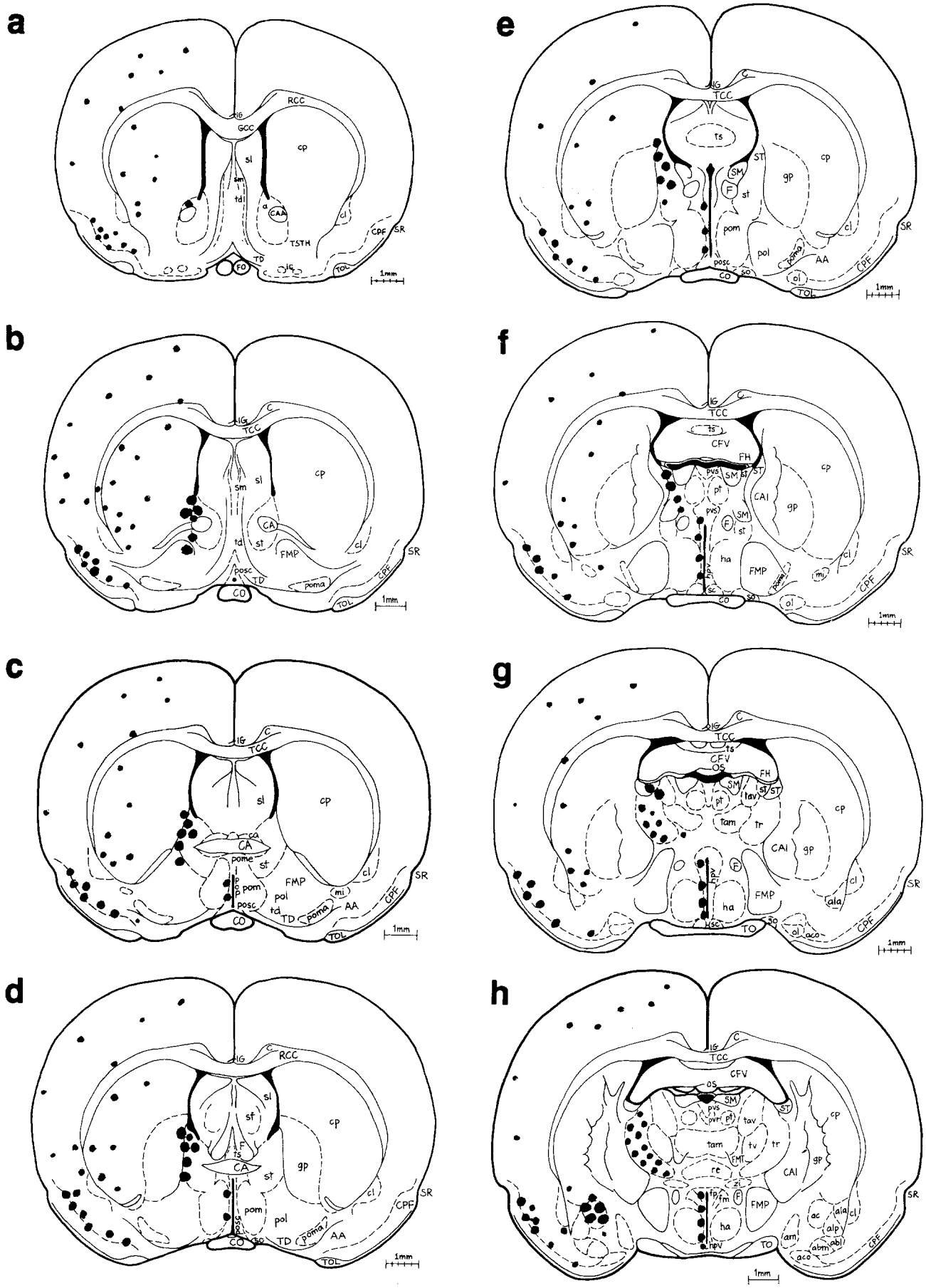

Fig. 33a–x (legend – see p. 403)

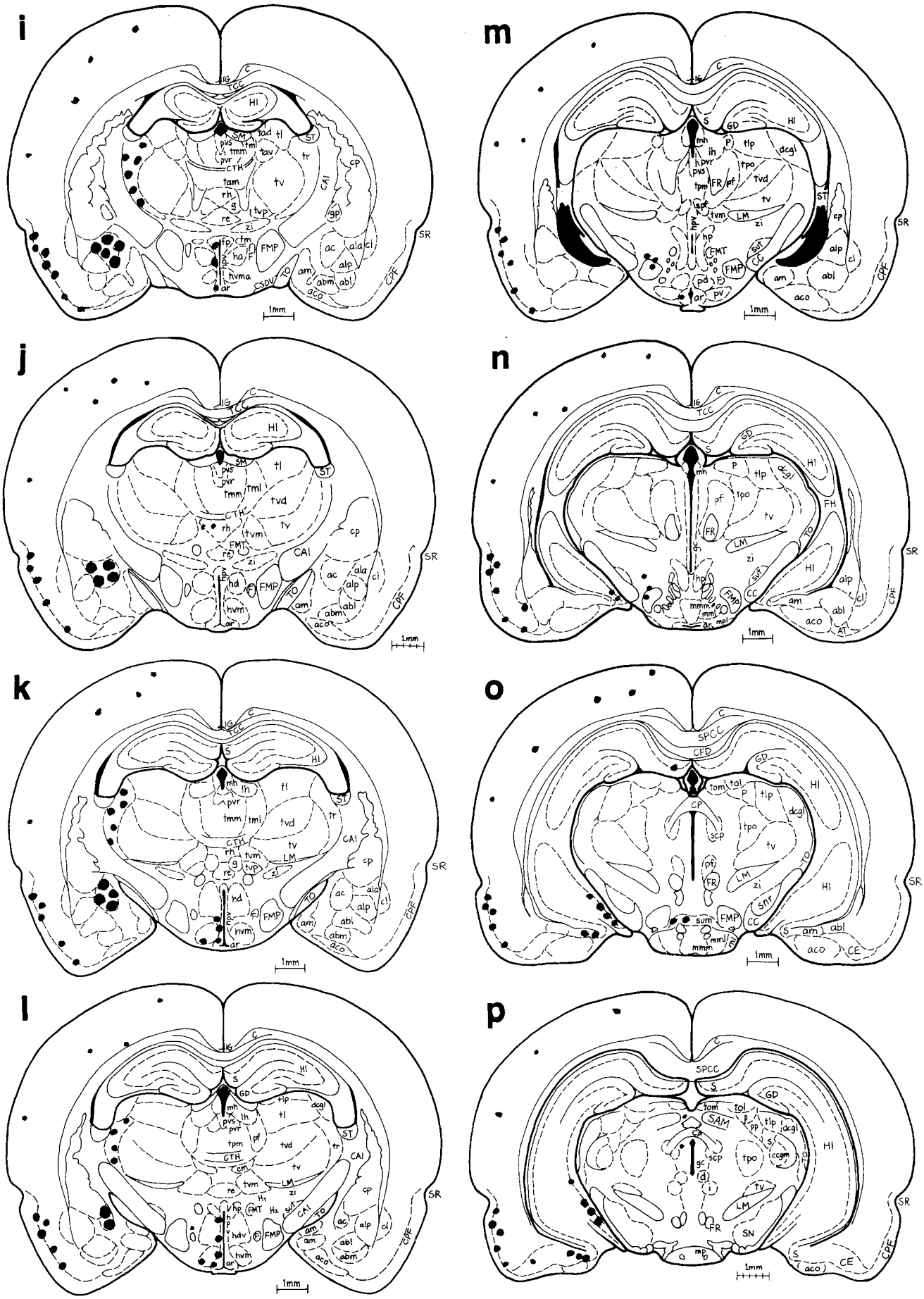

Fig. 33a–x (legend – see p. 403)

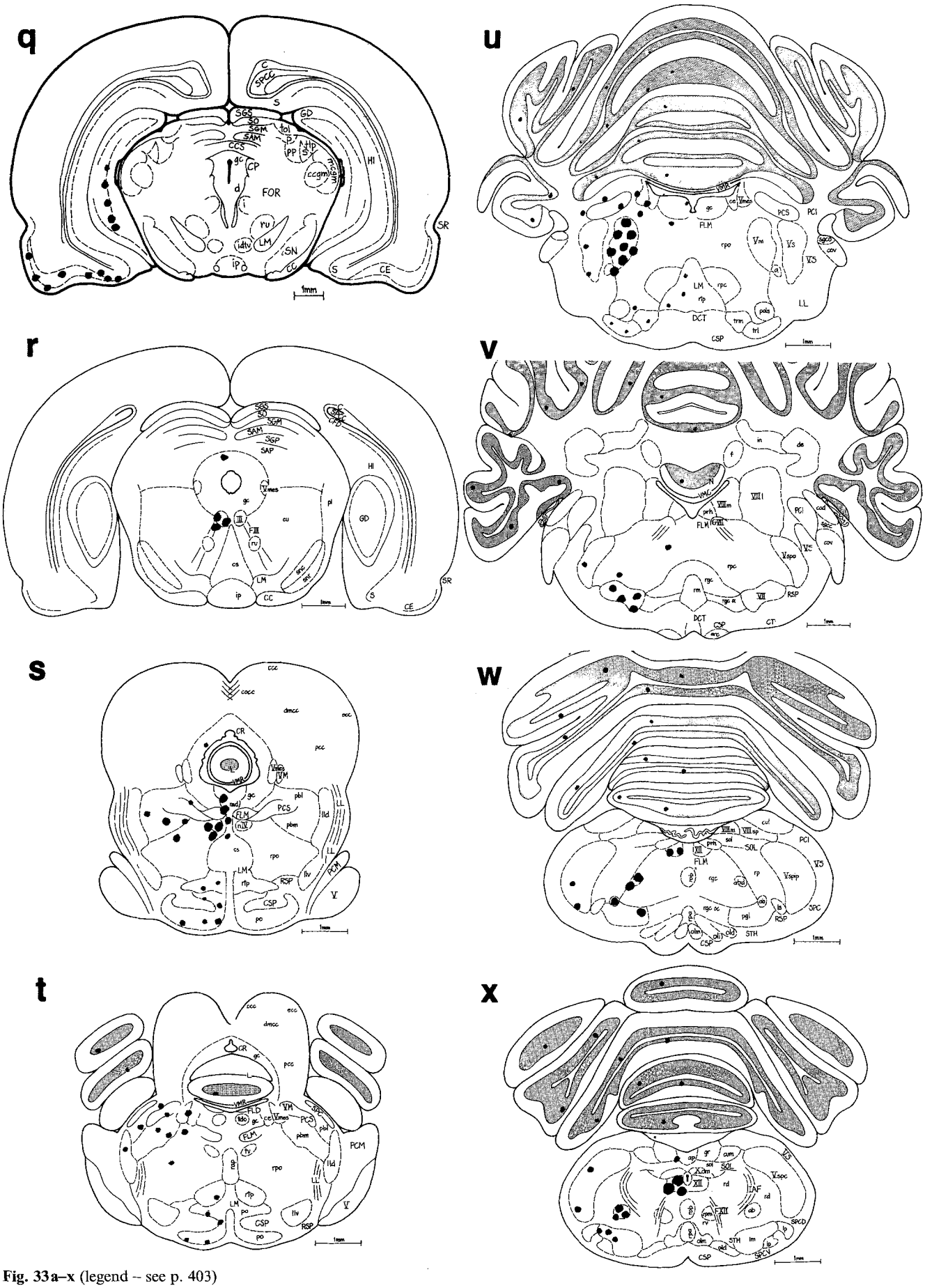

Fig. 33a–x (legend – see p. 403)

Fig. 33a–x. Brain distribution of target neurons for vitamin D. Frontal sections in rosto-caudal sequence, showing the topography of neurons with nuclear concentration of radioactivity after injection of ^{3}H 1,25 $(OH)_2$ vitamin D_3 (dots). Prepared after autoradiograms from adult mice. Size and frequency of dots correspond to intensity of nuclear labeling and frequency of occurence of labeled neurons. Designation of structures on right half

Abbreviations:

a	nucleus (n.) accumbens
AA	area amygdala anterior
aa	n. ambiguus
abl	n. amygdaloideus basalis
abm	n. amygdaloideus basalis pars medialis
ac	n. amygdaloideus centralis
aco	n.amygdaloideus corticalis
ala	n. amygdaloideus lateralis, pars anterior
alp	n. amygdaloideus lateralis, pars posterior
am	n. amygdaloideus medialis
ap	area postrema
ar	n. arcuatus hypothalami
C	cingulum
CA	commissura anterior
CAI	capsula interna
ccc	cortex colliculi caudalis
cl	claustrum
CO	chiasma opticum
COCC	commissura colliculi caudalis
cp	n. caudatus putamen
CPF	cortex piriformis
CR	recessus colliculi caudalis
cs	n. centralis superior
CSP	tractus corticospinalis
CTH	commissura thalami
cul	n. cuneatus lateralis
cum	n. cuneatus medialis
DCT	decussatio corporis trapezoidei
dmcc	n. dorsomedialis colliculi inferioris
ecc	n. externalis colliculi caudalis
F	columna fornicis
FLD	fasiculus longitudinalis dorsalis
FLM	fasiculus longitudinalis medialis
FMP	fasiculus medialis prosencephali
g	n. gelatinosus
gc	griseum centrale
gr	n. gracilis
hd	n. dorsomedialis hypothalami
HI	hippocampus
hpv	n. periventricularis hypothalami
hvm	n. ventromedialis hypothalami
IG	indusium griseum
L	lingula cerebelli
lh	n. habenulae lateralis
LL	lemniscus lateralis
lld	n. lemnisci lateralis dorsalis
llv	n. lemnisci lateralis ventralis
lm	n. reticularis lateralis magno cellularis
LM	lemniscus medialis
lp	n. reticularis lateralis parvo-cellularis
mh	n. medialis havenulae
old	n. olivaris accessorius dorsalis
oli	n. olivaris
olm	n. olivaris accessorius medialis
pbl	n. parabrachialis lateralis
pbm	n. parabrachialis medialis
pcc	n. principalis colliculi caudalis
PCM	pedunculus cerebellaris medius
PCS	pedunculus cerebellaris superior
po	n. pontis
pol	n. preopticus lateralis
pols	n. paraolivaris superior
pom	n. preopticus medialis
poma	n. preopticus magnocellularis
posc	n. preopticus, pars suprachiasmatica
pvr	n. periventricularis rotundo-cellularis
rad	n. raphes dorsalis
rap	raphes pontis
RCC	radiotio corpus callosi
re	n. reuniens
rgc	n. reticularis gigantocellularis
rh	n. rhomboideus
ro	n. Roller
rob	n. raphe obscurus
rp	n. reticularis parvocellularis
rpc	n. reticularis pontis caudalis
rpm	n. raphe paramedianus
rpo	n. reticularis pontis oralis
RSP	tractus rubrospinalis
rtp	n. reticularis tegmenti pontis
S	subiculum
sl	n. septi lateralis
sm	n. septi medialis
SOL	tractus solitarius
sol	n. tractus solitarii
SPCD	tractus spinocerebellaris dorsalis
ST	stria terminalis
st	n. interstitialis striae terminalis
STH	tractus spinothalamicus
TCC	truncus corporis callosum
td	n. tractus diagonalis (Broca)
tdo	n. tegmentalis dorsalis
tl	n. lateralis thalami
tml	n. medialis thalami, pars lateralis
tmm	n. medialis thalami, pars medialis
TO	tractus opticus
TOL	tractus olfactorius lateralis
tr	n. reticularis thalami
trl	n. trapezoides lateralis
trm	n. trapezoides medialis
tv	n. ventralis thalami
tvd	n. ventralis thalami, pars dorsomedialis
tvm	n. ventralis medialis thalami, pars magnocellularis
tvp	n. ventralis medialis thalami, pars parvocellularis
V	nervus trigeminus
VM	tractus mesencephalicus nervi trigemini
Vm	n. motorius nervi trigemini
Vmes	n. tractus mesencephali nervi trigemini
VMR	velum medullare rostralis
VS	tractus spinalis nervi trigemini
Vs	n. sensibilis nervi trigemini
Vspc	n. caudalis tractus spinalis nervi trigemini
Xdm	n. dorsalis motorius nervi vagi
XII	n. nervi hypoglossi
FXII	fibrae nervi hypoglossi

Most of the cells in the autonomic motor nucleus ambiguus show a nuclear concentration of radioactivity (Fig. 29). In the nucleus sensibilis of the trigeminus, as in the caudally connected substantia gelatinosa, small labeled neurons are scattered among unlabeled cells. A small group of medium-sized labeled neurons exists in the region of the nucleus reticularis lateralis magnocellularis. On occasion a few small labeled cells are noted in the vicinity of the area postrema, while the nucleus tractus solitarii and the adjacent nucleus of the vagus nerve are free of labeled cells (Fig. 32).

In the cerebellum, in most of the animals no nuclear labeling is observed. The exception are the animals that received the highest dose of ^{3}H 1,25 D_3, in which a distinct nuclear concentration of radioactivity can be noted in a number of Golgi type II neurons (Figs. 27 and 28). Purkinje cells, basket cells and granule cells remain unlabeled.

A quantitative evaluation of radiolabeled molecules per nucleus was done in select structures in the adult female Swiss Webster mouse which had a normal diet, injected with a dose of 0.38 µg/100 g b.w. of ^{3}H 1,25 D_3 and sacrificed 3 h afterwards. For radiolabeled molecules per cell nucleus, and for the ratio of numbers for the mean values with standard error and for the labeling indices, the data are as follows: bed nucleus of the stria terminalis, pars lateralis, 6108 ± 374 (21%); central nucleus of the amygdala, 6102 ± 870 (14%); caudate-putamen, regio ventrolatealis, 2907 ± 420 (31%); cerebellum, Golgi type II cells, 2829 ± 262 (41%); cortex piriformis, lamina II, 780 ± 99 (17%); non-neural tissues for comparison: pituitary (thyro-

tropes), 4486±370 (5–9%); duodenum intervillous crypts, 4026±295 (90–95%). Results from the adult male Swiss Webster mouse with identical treatment are: duodenum intervillous crypts, 4287±249 (90–95%): pituitary (thyrotropes), 4419±449 (5–9%); nucleus nervi trigemini motor, 5912±694 (64%); small labeled cells in the region of the locus ceruleus and nucleus parabrachialis, 3588±354 (12%).

In an adult male Sprague Dawley rat that was kept on a vitamin D deficient diet, injected i.v. with a low dose of 0.05 μg/100 g b.w. of ^{3}H 1,25 D_3 and killed 2 h afterwards, the following counts were obtained: duodenum intervillous crypts, 1843±192 (71%); central nucleus of the amygdala, 2265±196 (8%); bed nucleus of the stria terminalis, pars lateralis, 2340±450 (6%).

Discussion

The results presented here extend those from our earlier publications on 1,25 $(OH)_2$ vitamin D_3 nuclear receptors in the nervous system (Stumpf et al. 1979, 1980). Our discoveries of the brain and pituitary as targets for calcitriol were largely unexpected by those working with this hormone. Even to date, there is no evidence from biochemical studies that would support our findings, and the published results about cytosolic or nuclear specific binding in the brain are negative (Colston et al. 1980). The situation is reminiscent of the discovery of progestin nuclear binding in the brain through the use of autoradiography (Sar and Stumpf 1973). For five subsequent years, investigators that used disruptive biochemical approaches were unable to provide evidence for specific nuclear binding. When a more refined and careful dissection of brain regions rich in target cells was employed, based on the autoradiographic data, specific receptor binding was demonstrated.

As is the case with other steroid hormones (Stumpf and Sar 1976), calcitriol target cells are found in many diverse organs and in many regions of the brain. In the brain, the topographical distribution of target cell groups suggests a pattern that relates to neuronal circuits. It suggests further that 1,25 D_3 addresses neurochemically and functionally heterogeneous populations. While such apparent diversity may seem confusing, it is likely to represent a means for functional coordination and integration, as is apparent with other steroid hormones (Stumpf and Jennes 1984). For instance, ^{3}H estradiol has been reported to concentrate in neurons in the diencephalon that correspond to projection sites of the stria terminalis (Stumpf 1968). In subsequent studies, additional projection sites were implicated and the concept of estrogen-neuron systems in the brain was proposed (Stumpf 1970). The additional observation of regional differences in the intensity of nuclear estradiol binding, in conjunction with evidence for diverse effects on brain functions, led to the development of the concept of MAHS, an acronym for Multiple Activation of Heterogeneous Systems (Stumpf and Sar 1981). This concept implies that steroid hormones activate simultaneously and differentially a number of functionally defined systems. It is further implied from observations about quantitative variations of nuclear uptake that hormonal responses can selectively change, so that at a certain endocrine status stimulatory responses predominate, while ensueing changes of hormone levels and related changes in hormone binding, may result in the predominance of inhibitory responses. With the data now available on calcitriol, it is proposed that the same applies to this "calcium homeostatic" hormone.

Prelimary quantitative data on nuclear uptake and retention of ^{3}H 1,25 D_3 indicate that the number of nuclear molecules is highest in certain neurons in a subsystem of the stria terminalis. This involves the dorsolateral bed nucleus of the stria terminalis and the central nucleus of the amygdala. In these neurons, as well as in neurons of cranial motor nerves, the highest nuclear content of radioactivity was observed with about 6000 radiolabeled molecules per nucleus. This was somewhat higher than in pituitary thyrotropes and in epithelial crypt cells in the duodenum. Much lower numbers of about 1000–3000 molecules per nucleus were computed for cerebellar Golgi type II cells, neurons on the caudate-putamen, and neurons in the piriform cortex. The number of nuclear molecules in target cells was, in general, lower in animals which had received a relatively low dose of radiolabeled hormone, indicating that probably only a portion of the binding sites was occupied. This assumed relationship between administered dose and receptor occupancy, and similar influences of age, diet, time interval after the injection, and others, need to be studied with larger numbers of animals for statistical evaluation. Clarification is also needed for the negative or low nuclear and high cytoplasmic radioactivity noted in large neurons. This may indicate for certain cells a presence of a cytoplasmic-nuclear barrier and a binding of the hormone to cytoplasmic protein or organelles.

Our results suggest that vitamin D strongly affects motor functions and that its well known effects on muscle physiology are mediated predominantly through genomic 1,25 D_3 actions on motor neurons, in addition to indirect actions through blood calcium levels, but not through direct genomic 1,25 D_3 actions on skeletal muscle, since no evidence for nuclear binding has been seen in autoradiograms of skeletal muscle from animals that showed nuclear binding of ^{3}H 1,25 D_3 in motor neurons, as well as in epithelium of intestine and kidney tubules, osteoblasts, and other target tissues. Modulations of extrapyramidal and cerebellar motor functions may be expected through target cells in the caudate-putamen, the nucleus pontis, and the Golgi type II cells in the cerebellum. Target neurons in the substantia gelatinosa of the spinal cord and medulla oblongata as well as in the ganglion of the trigeminus (Stumpf et al. 1987a), suggest effects on tactile or pain perception. The strongly suggested influence of 1,25 D_3 on thalamic integration and activation through actions on the nucleus reticularis thalami, urges further investigation. The target neurons in the parabrachial region, although small in number, are likely to affect gustatory and certain autonomic functions. Autonomic intestinal influences may be exerted through target neurons in the nucleus ambiguus and, perhaps, the central nucleus of the amygdala together with the dorsolateral bed nucleus of the stria terminalis. While the target neurons in the latter nuclei may be neurotensinergic, involvement of serotonin, dopamine, and TRH neuronal systems is also suggested through localization elsewhere. In the central hypothalamus, target neurons are present in the dorsal arcuate and ventral periventricular nuclei, the region were dopaminergic neurons are located. TRH, but also CRF, somatostatin and other hormones, are found in the periventricular nucleus at the anterior hypothalamic level including the parvocellular paraventricular nucleus. It is possible, that 1,25 D_3 modulates TRH secretion through these neurons

for "feed-back" regulation of a hypothesized vitamin D dependent Brain-Pituitary-Thyroid Axis. The existence of a brain-pituitary endocrine axis for vitamin D, analogous to other steroid hormones, has been postulated earlier (Stumpf et al. 1982) in view of our localization data as well as effects of calcitriol on the secretion of TSH (Sar et al. 1981) and of insulin (Clark et al. (1981). The presence of 1,25 D_3 target neurons in the arcuate nucleus, ventromedial nucleus, periventricular nucleus and of target cells in reproductive organs, suggests further effects of vitamin D_3 on the regulation of reproduction.

Vitamin D dependent changes in brain calcium binding protein have been reported in chicken (Taylor and Brindak 1974; Jande et al. 1981) and in mammals (Baimbridge and Miller 1982; Feldman and Christakos 1983; Garcia-Segura et al. 1984; Parkes et al. 1985). In these studies, vitamin D dependent calcium binding protein has been shown to exist in many brain regions, that include glial and ependymal cells, neurons in the cortex, and especially Purkinje cells in the cerebellum. In a comparative study with antibodies to vitamin D dependent calcium binding protein and antibodies to 1,25 D_3 receptor (Clemens et al. 1985), calcium binding protein was found strongest in the cerebellum in Purkinje cells and was low in granule cells, while receptor immunoreactivity was "completely absent in Purkinje cells but was found instead in the immediately adjacent granule cell nuclei". In the same study, in the dorsal hippocampus, the pattern of staining of calcium binding protein was stated to be "strikingly similar to that of the 1,25 D_3 receptor", although the published pictures do not convey such correspondence. The results of Clemens et al. are at variance not only regarding sites of "receptor" staining and calcium binding protein localization, but also with respect to our localization of the hormone.

In the brain, there is in general a very limited correspondence between the localization of tritium-labeled 1,25 D_3 and the localization of antibodies to 28 k vitamin D dependent calcium binding protein. Such discrepancies have been observed earlier with other calcitriol target tissues as defined by autoradiography, including intestine, endocrine pancreas, skin, adrenal medulla, placenta, and pituitary. Therefore, vitamin D dependent calcium binding protein may be a product of calcitriol genomic stimulation only in certain tissues, while in others, the major product may be a cell-type specific response as diverse as TSH secretion (Sar et al. 1981), insulin secretion (Clark et al. 1981), gastrin secretion (Stumpf et al. 1979), proliferation and maturation of skin (Hosomi et al. 1983) and probably many others. Despite these and other apparently diverse actions of vitamin D, many of the seemingly unrelated actions may be integrative and subserving the goal to assure calcium equilibrium and skeletal growth and maintenance.

However, the presence of nuclear receptors for 1,25 D_3 in many regions of the central nervous system, in pituitary cells, and in a multitude of peripheral organs, in conjunction with related known or postulated functions, demands a revision of the current and classical concepts of vitamin D action. Vitamin D is much more than "the calcium homeostatic steroid hormone".

In the light of extensive new information foremost derived from the results of our autoradiographic and histochemical studies, it appears that 1,25 D_3, is a comprehensive biological activator and regulator of vital systems. Vitamin D_3 mediated activation is purposefully linked to and in tune with the exposure to the seasonal rise of the sun with the apparent goal of environment-linked optimized regulation of development, maintenance and propagation of life. This involves proliferation and maturation of certain tissues, calcium homeostasis and muscular eutrophy for skeletal strength and movement, sensitation, and, ultimately, facilitation of reproduction.

Regulation of calcium metabolism is one, but only one, important component of vitamin D_3 action. "Calcitriol" may more appropriately be termed solitriol, the sunlight related steroid hormone, the seasonal activator and regulator, the somatotrophic heliogenic steroid messenger.

Acknowledgement. Supported in part by USPHS grants NS 09914 and HD 03110.

References

Baimbridge KG, Miller JJ (1982) Immunohistochemical localization of calcium-binding protein in the cerebellum, hippocampal formation and olfactory bulb of the rat. Brain Res 245:223–229

Clark SA, Stumpf WE, Sar M, DeLuca HF, Tanaka Y (1980) Target cells for 1,25 dihydroxyvitamin D_3 in the pancreas. Cell Tissue Res 209:515–520

Clark SA, Stumpf WE, Sar M (1981) Effect of 1,25 dihydroxyvitamin D_3 on insulin secretion. Diabetes 30:382–386

Clark SA, Stumpf WE, Bishop CW, DeLuca HF, Park DH, Joh TH (1986) The adrenal: A new target organ of the calciotropic hormone 1,25-dihydroxyvitamin D_3. Cell Tissue Res 243:299–302

Clemens TL, Zhou XY, Pike JW, Haussler MR, Sloviter RS (1985) 1,25 Dihydroxyvitamin D receptor and vitamin D– dependent calcium-binding protein in rat brain: comparative immunocytochemical localization. In: Norman AW, Schaefer K, Grigoleit H-G, Herrath Dv (eds) Vitamin D. A chemical, biochemical and clinical update. Walter de Gruyter, Berlin, pp 95–96

Colston K, Hirst M, Feldman D (1980) Organ distribution of the cytoplasmic 1,25 dihydroxcholecalciferol receptor in various mouse tissues. Endocrinology 107:1916–1922

Feldman SC, Christakos S (1983) Vitamin D-dependent calcium-binding protein in rat brain: biochemical and immunohistochemical characterization. Endocrinology 112:290–302

Garcia-Segura LM, Baetens D, Roth J, Norman AW, Orci L (1984) Immunocytochemical mapping of calcium-binding protein immunoreactivity in the rat central nervous system. Brain Res 296:75–86

Gascon-Barré M, Huet PM (1983) Apparent [^{3}H] 1,25-dihydroxyvitamin D_3 uptake by canine and rodent brain. Am J Physiol 244:E266–E271

Hosomi J, Hosoi J, Abe E, Suda T, Kuroki T (1983) Regulation of terminal differentiation of cultured mouse epidermal cells by 1,25-dihydroxyvitamin D_3. Endocrinology 113:1950–1957

Jande SS, Maler L, Lawson DEM (1981) Immunohistochemical mapping of vitamin D-dependent calcium-binding protein in brain. Nature 294:765–767

Parkes CO, Mariani J, Thomasset M (1985) 28-kDa Cholecalcin (CaBP) levels in cerebella of mutant mice. In: Norman AW, Schaefer K, Grigoleit H-G, Herrath Dv (eds) Vitamin D. A chemical, biochemical and clinical update. Walter de Gruyter, Berlin, pp 359–360

Sar M, Stumpf WE (1973) Neurons of the hypothalamus concentrate ^{3}H progesterone or metabolites of it. Science 182:1266–1268

Sar M, Stumpf WE, DeLuca HF (1980) Thyrotropes in the pituitary are target cells for 1,25 $(OH)_2$ vitamin D_3. Cell Tissue Res 209:161–166

Sar M, Miller WL, Stumpf WE (1981) Effects of 1,25 $(OH)_2$ vitamin D_3 on thyrotropin secretion in vitamin D deficient male rats. Physiologist 24:70

Sonnenberg J, Luine VN, Krey LC, Christakos S (1986) 1,25 Di-

hydroxyvitamin D_3 treatment results in increased choline acetyltransferase activity in specific brain nuclei. Endocrinology 118:1433–1439

Stumpf WE (1968) Estradiol concentrating neurons: Topography in the hypothalamus by dry-mount autoradiography. Science 162:1001–1003

Stumpf WE (1970) Estrogen-neurons and estrogen-neuron systems in the periventricular brain. Am J Anat 129:207–218

Stumpf WE (1976) Techniques for the autoradiography of diffusible compounds. In: Prescott DM (ed) Methods in cell biology, vol XIII. Academic Press, New York, pp 171–193

Stumpf WE, Jennes L (1984) The A-B-C (Allocortex-Brainstem-Core) circuitry of endocrine-autonomic integration and regulation. Relationships between estradiol sites of action and peptidergic-aminergic neuronal systems. In: Brain-Endocrine Symposium V, Würzburg, Peptides 5 (Suppl) 1:221–226

Stumpf WE, O'Brien LP (1987) Autoradiographic studies with ^3H 1,25-dihydroxyvitamin D_3 in thyroid and associated tissues of the neck region. Histochemistry 87:53–58

Stumpf WE, Roth LJ (1966) High resolution autoradiography with dry-mounted, freeze-dried, frozen sections. Comparative study of six methods using two diffusible compounds, ^3H-estradiol and ^3H-mesobilirubinogen. J Histochem Cytochem 14:274–287

Stumpf WE, Sar M (1976) Autoradiographic localization of estrogen, androgen, progestin, and glucocorticosteroid in "target tissues" and "non-target tissues". In: Pasqualini J (ed) Receptors and mechanism of action of steroid hormones. Modern pharmacology-toxicology, vol 8. Marcel Dekker, New york, pp 41–84

Stumpf WE, Sar M (1981) Anatomical relationships between estrogen target sites and peptidergic-aminergic neurons: Multiple activation of heterogeneous systems (MAHS). Exp Brain Res Suppl 3:18–28

Stumpf WE, Sar M, Grant LD, Heritage AS (1978) Periventricular secretory units: Sites of sex steroid hormone action, neurohormone production and secretion. In: Scott DE, Koslowski GP,Weindl W (eds) Brain-endocrine interaction III. Neural hormones and reproduction. S Karger, Basel, pp 212–227

Stumpf WE, Sar M, Reid FA, Tanaka Y, DeLuca HF (1979) Target cells for 1,25-dihydroxyvitamin D_3 in intestinal tract, stomach, kidney, skin, pituitary, and parathyroid. Science 206:1188–1190

Stumpf WE, Sar M, Clark SA, Lieth E, DeLuca HF (1980) Target neurons for 1,25-dihydroxyvitamin D_3 in brain and spinal cord. Neuroendocrinol Lett 2:297–301

Stumpf WE, Sar M, DeLuca HF (1981a) Sites of action of 1,25 $(OH)_2$ vitamin D_3 identified by thaw-mount autoradiography. In: Cohn DV, Talmage RV, Matthews JL (eds) Hormonal control of calcium metabolism. Excerpta Medica, Amsterdam, pp 222–229

Stumpf WE, Sar M, Zuber TJ, Soini E, Tuohimaa P (1981b) Quantitative assessment of steroid hormone binding sites by thaw-mount autoradiography. J Histochem Cytochem 29:1A:201–206

Stumpf WE, Sar M, Clark SA, DeLuca HF (1982) Brain target sites for 1,25-dihydroxyvitamin D_3. Science 215:1403–1405

Stumpf WE, O'Brien LP, Morin J, Reid FA (1987a) Target neurons for 1,25 $(OH)_2$ vitamin D_3 in spinal cord and trigeminal ganglion. Anat Embryol (in press)

Stumpf WE, Sar M, Chen K, Morin J, DeLuca HF (1987b) Sertoli cells in the testis and epithelium of the ductuli efferentes are targets for ^3H 1,25 dihydroxyvitamin D_3. Cell Tissue Res 247:453–455

Taylor AN, Brindak ME (1974) Chick brain calcium-binding protein: comparison with intestinal vitamin D-induced calcium binding protein. Arch Biochem Biophys 161:100–108